Nanoscale Horizons

Accepted Manuscript

Volume 1 | Number 1 | January 2016 | Pages 1–82

Nanoscale Horizons

The home for rapid reports of exceptional significance in nanoscience and nanotechnology
rsc.li/nanoscale-horizons

ISSN 2055-6756

COMMUNICATION
Shi Zhang Qiao et al.
Three dimensional nitrogen-doped graphene hydrogels with in situ deposited cobalt phosphate nanoclusters for efficient oxygen evolution in a neutral electrolyte

ROYAL SOCIETY
OF CHEMISTRY

rsc.li/nanoscale-horizons

1

Primary microglia maintain capacity to function despite internalisation and intracellular loading with carbon nanotubes

Cyrill Bussy[1,*], Alberto Bianco[2], Maurizio Prato[3,4,5] and Kostas Kostarelos[1,*]

[1] Nanomedicine Lab, Faculty of Biology, Medicine and Health & National Graphene Institute, University of Manchester, AV Hill Building, Manchester M13 9PT, United Kingdom

[2] CNRS, Institut de Biologie Moléculaire et Cellulaire, UPR 3572, Immunopathologie et Chimie Thérapeutique, Strasbourg, France

[3] Center of Excellence for Nanostructured Materials, Department of Chemical and Pharmaceutical Sciences, University of Trieste, Trieste, Italy

[4] Carbon Nanobiotechnology Laboratory, CIC biomaGUNE, Paseo de Miramón 182, 20009 Donostia-San Sebastian , Spain

[5] Basque Science Foundation, Ikerbasque, Bilbao 48013, Spain

* Corresponding to: cyrill.bussy@manchester.ac.uk; kostas.kostarelos@manchester.ac.uk

1

1 # Abstract

2

3 Biomedical applications of functionalised carbon nanotubes (*f*-CNTs) for imaging as well as
4 drug or gene delivery in the brain have recently gained interest. Several studies have
5 demonstrated the potential of *f*-CNTs to offer treatment options for neurological conditions
6 with success. However, there is also evidence that *f*-CNTs accumulate preferentially within
7 microglial cells when introduced in the brain. Considering the key immunologic role of these
8 cells in the brain and the limited knowledge regarding the interaction of CNTs with microglial
9 cells, it is imperative to understand whether accumulation of CNTs in microglial cells can
10 alter their physiological functions or trigger pro-inflammatory signalling. The aim of the
11 present study was to investigate the basic physiological functions of isolated primary
12 microglial cells over time, following their exposure to multi-walled carbon nanotubes
13 functionalized via different surface chemistries. We rationalized that some chemical
14 strategies may be more deleterious for microglial cell functions than others. We used rat
15 primary microglial cells that can be maintained in cell culture for a long period of time without
16 undergoing cell division. Cell viability, phagocytosis, migration, pro-inflammatory factor
17 release were studied over one month, following a single exposure to a non-cytotoxic
18 concentration of three different *f*-CNTs (carboxylated, aminated and both carboxylated and
19 aminated). We show that *f*-CNTs do not induce inflammation and are not affecting basic
20 functions of microglial cells under these conditions. Importantly, this was the case from day 1
21 to day 28 post-exposure, even though microglial cells had internalized *f-C*NTs in subcellular
22 compartments and retained the nanotube load in their cytoplasm over time.

23
24
25
26
27 ## Key words
28 nanomedicine; brain; biocompatibility; central nervous system; phagocytosis; neurotoxicity; nanotoxicology
29
30

Introduction

In recent years, numerous nanomaterials have been utilised in an attempt to overcome the great challenge of drug delivery to the central nervous system [1-3]. Among them, carbon nanotubes (CNTs) have lately shown great promise [4] due to their inherent properties, but also a unique ability to cross cellular barriers [5]. For instance, acetylcholine adsorbed onto single-walled CNTs (SWNTs) was efficiently delivered to cells in a kainic acid induced Alzheimer's Disease (AD) mouse model [6]. Amine functionalized multi-walled CNTs (MWNTs) have also been used successfully to deliver Caspase 3 siRNA into neurons with the aim to reduce the ischemic injuries in the motor cortex of an endothelin-1 induced stroke model [7]. Similarly, amine functionalized SWNTs were injected in mouse brain ventricles in order to decrease the effects of ischemia and inflammation in an artery occlusion model of stroke [8]. The SWNT treated animals showed better histopathological and behavioural profiles after injury, indicating that aminated SWNTs could achieve a neuroprotective effect even without carrying any therapeutic agent. More recently, PEG-SWCNTs have also been proposed as solutions to alleviate glutamate excitotoxicity of neurons by increasing astrocytic glutamate uptake [9].

Once localised in the brain parenchyma, knowledge of the fate and biological effects of those functionalised nanomaterials remains however limited. This raises the need for a better understanding of the interactions of carbon nanomaterials with the different cell subpopulations in the central nervous system (CNS). While neurons might be a preferred target for therapeutic purposes, nanomaterial in the brain parenchyma are likely to interact with other cell types including the resident macrophages of the brain, namely the microglial cells. Even in the case of nanoscale vectors bearing neuron-targeting moieties, microglial cells have indeed been shown to be the cell type in which a significant fraction of the nanomaterials were accumulating [10]. Considering that microglial cells are the main cellular component of the immune system in the brain, any nanomaterial that is intended for intracerebral applications should therefore have a controlled and well-understood interaction with those cells.

In terms of our current understanding of CNT-microglia interactions, microglial cells have been reported to play a major role in internalising functionalised CNTs (*f*-CNTs) in comparison to other cell types following stereotactic administration of *f*-CNT in the cortex of mice [7, 11, 12]. Similar results were obtained *in vitro* in mixed cell culture of primary glial cells, whereby microglial cells were displaying higher uptake of functionalised MWNTs (*f*-MWNTs) compared to astrocytes [13]. Interestingly, following internalisation in microglial cells, we have observed the partial degradation of *f*-MWNTs over time, both *in vivo* over 14 days [12] and *in*

1 *vitro* in a primary cell culture model up to 90 days [14, 15]. Alteration within 24h of the graphitic

2 structure of *f*-MWNTs in the immortalised N9 microglial cell line offered independent

3 validation [16].

4 These degradation results suggested that despite the internalisation of *f*-CNTs,

5 microglial cells were able to maintain one of their primary functions over time: their ability to

6 degrade foreign materials [12, 14, 17]. In contrast, MWNTs dispersed in horse serum were shown

7 *in vitro* to alter microglial functions such as migration and phagocytosis, and also cell division

8 in BV2 immortalised microglial cell model after their internalisation[18]. The main hypothesis to

9 explain these alterations was the direct interaction of MWNTs with the cytoskeleton of BV2

10 cells leading to an impairment of all cytoskeleton related functions including migration and

11 phagocytosis. The present study was therefore designed to interrogate the impact of

12 internalisation and retention of *f*-CNTs in microglial cells on their capacity to perform normal

13 cellular and macrophage-specific functions, other than their degradation ability that was

14 previously demonstrated [14, 15].

15

16 In addition, using different chemical derivatives of *f*-CNTs, surface properties have

17 been revealed as essential determinants that could modulate both CNT-microglia interaction

18 and bioreactivity of CNTs towards microglial cells. Firstly, the type of surface functionalisation

19 was demonstrated to influence the uptake[19]. Phosphatidyl-serine coated SWNTs were

20 engulfed by primary rat microglia while phosphatidyl-choline coated and non-coated SWNTs

21 were not. Similarly, microglial cells were shown to be very efficient at internalising oxidised

22 MWNTs but were not fully able to break apart agglomerates of pristine MWNTs and to

23 internalise them [16]. Secondly, the type of functionalisation was shown to modulate the

24 response of microglial cells. While both pristine and oxidised MWNTs were not altering cell

25 viability, pro-inflammatory cytokine release or nitric oxide (NO) production, a significant

26 increase of reactive oxygen species production was measured after exposure to pristine

27 MWNTs, suggesting possible impact on cell viability at long term [16]. Accordingly, using an *in*

28 *vivo* cortical stereotactic injection model, brain cells and microglial ones in particular were

29 reported to differently respond to *f*-CNTs exposure depending on the surface

30 functionalisation of the materials injected [11]. Functionalisation was not only impacting the

31 localisation and distribution pattern of the injected materials within the brain, but also

32 modulating the inflammatory profile of the different *f*-CNTs. Oxidised MWNTs were shown to

33 induce and sustain a microglial cell mediated inflammatory response while aminated MWNTs

34 were only transiently inducing inflammation.

35 Taken together, these studies demonstrate the major importance of material surface

36 properties and in particular the type of surface functionalisation on the biological outcomes of

37 the material-cell interaction. Moreover, ability by CNTs to induce inflammation and impact on

1 microglial cell physiological functions are two key endpoints that should be systematically
2 investigated and correlated to the surface chemistry of the materials in order to determine the
3 best biocompatibility profile for putative CNT-based brain delivery systems.
4

5   The objectives of the present study were therefore to investigate whether microglial
6 cell functions can be affected by the internalisation of *f*-CNTs, whether varying the surface
7 chemistry of *f*-CNTs can modulate the cell response, and whether the impact of these
8 different *f*-CNTs on microglial cell functions may evolve over time. Oxidation of CNTs has
9 been shown to increase the bioreactivity of those materials for macrophages [11, 20], we
10 therefore hypothesised that the degree of oxidation/carboxylation is determinant to modulate
11 the biological responses and can affect microglial cell functions while not inducing cell death.
12 To assess this hypothesis we selected three MWNTs with different carboxylation degree
13 (purely carboxylated, purely aminated and one type baring both carboxyl and amine groups).
14 We additionally developed a primary rat microglial cell model that demonstrated a long
15 lifespan *in vitro* without undergoing division to monitor over time the evolution of microglial
16 cell functions after internalisation of the materials. Cytotoxicity, phagocytosis, migration and
17 pro-inflammatory mediator release were studied at different time points and up to 28 days
18 following a single exposure to a non-cytotoxic concentration of the three selected *f*-CNTs.
19 We report that *f*-MWNTs irrespective of their chemical functionalisation did not affect
20 microglial cell viability under our conditions and did not induce release of pro-inflammatory
21 mediators at any time points. Moreover, despite an important perinuclear internalisation of
22 materials, microglial cells maintained their abilities to phagocytose and to migrate.
23 Interestingly, oxidation of MWNTs stimulated the migration ability of microglial cells that have
24 engulfed those CNTs in comparison to aminated MWNT laden cells.
25

Results and Discussion

27 **Chemical structure and characterisation of MWNT suspension.** The selection of
28 MWCNTs over other CNT types such as single walled- or double walled- CNTs was
29 motivated by our previous works on the interactions of *f*-MWNTs with brain cells [7, 11-13, 21] and
30 microglial cells in particular [14, 15]. We have also demonstrated that these functionalised
31 nanomaterials can be used as delivery platforms for drugs [22], genes [7, 23] or contrast agents [24].
32 The type of chemical functionalisation was previously identified by some of us as a major
33 determinant of the *in vivo* ability of *f*-MWNTs to induce inflammation in the brain [11].
34 Comparing two types of *f*-MWNTs, one that has been pre-oxidised and then aminated with
35 one that has been aminated only, oxidation/carboxylation was revealed as causing
36 inflammation, even though the effects of MWNTs bearing only carboxyl groups (i.e. negative

1 charges) were not directly investigated. Here, three chemically functionalised MWNTs with

2 different level of oxidation were synthesised from the same starting materials in order to limit

3 batch-to-batch variations. Their chemical structure is presented in **Figure 1** and they include:

4 *(i)* carboxylated MWNTs (ox-MWNTs) prepared by treatment of the starting materials in

5 strong acid conditions [25]; *(ii)* amino-functionalized oxidised MWNTs (ox-MWNT-NH_3^+)

6 prepared by 1,3 dipolar-cycloaddition reaction after an initial oxidation as described

7 previously [26]; and *(iii)* amino-functionalized MWNTs (MWNT-NH_3^+) prepared following the 1,3

8 dipolar-cycloaddition reaction on the starting materials as described previously [27, 28]. Length

9 of MWNT-NH_3^+ remained similar to the one of the starting materials (between 0.5-2 μm)

10 while it was reduced for materials undergoing oxidation (shorten to 300-400nm for ox-MWNT

11 and ox-MWNT-NH_3^+). Suspensions of MWNTs were prepared by hydrating dry powder with a

12 5% dextrose water solution, which was then sonicated until MWNTs reached a good

13 dispersion (about 40 min). It was essential to achieve a dispersion of similar quality for the

14 three materials to prevent non-intrinsic differences amongst them. Difference in dispersion

15 quality is indeed known to induce differences in biological responses especially inflammation

16 [29, 30] and could therefore lead to biases in experiment outcomes and misinterpretation in

17 regards to the role of chemical functionalisations. To assess the stability of the 3 MWNT

18 dispersions in 5% dextrose water solution, analysis of the absorbance (used as an index of

19 dispersion, well dispersed materials absorbing more than agglomerated ones) was

20 performed at 0 h and 24 h (**Figure S1**, first column). Despite the intrinsic differences between

21 the 3 materials (highest absorbance: ox-MWNT-NH_3^+ > MWNT-NH_3^+ > ox-MWNT), no

22 difference between the absorbances at 0 h and 24 h could be observed for any materials. All

23 3 materials were stable over 24 h in 5% dextrose. Similar stability results over 24 h were

24 observed when the materials initially suspended in 5% dextrose were diluted in cell culture

25 medium supplemented with 12% FBS (**Figure S1**, second column). However, when

26 materials initially suspended in 5% dextrose were then diluted in cell culture medium without

27 FBS, the UV-Vis spectrometric analysis evidenced a clear sedimentation for all 3 materials,

28 regardless of their surface chemistries (**Figure S1**, third column). These results suggested

29 that MWNT suspensions were not stable in cell culture medium without the addition of FBS,

30 and would sediment at the bottom of the cell culture wells under these conditions, increasing

31 the potential of materials to interact with the monolayer of cells. In contrast the addition of

32 FBS would not be favourable to interaction with cells as most materials would stay in

33 suspension, above the cell monolayer.

34 **Functionalised nanotubes had no effect on microglial cell viability.** Microglial cells were

35 revealed as the main cell population in which *f*-MWNTs are accumulating when infused in the

36 brain parenchyma [7, 11, 12], or when exposing mixed glial cells cultures (containing mainly

1 astrocytes and microglial cells) [13, 14]. However, the impact of this preferential accumulation

2 remains elusive and contradictory in the literature. We therefore first questioned whether the

3 exposure to different *f*-MWNTs using a non-overload concentration will affect the viability of

4 microglial cells over time. To answer that question, a model of primary microglial cell cultures

5 that can be maintained over long period of time without cell division was used. It was

6 rationalised that once in the brain parenchyma, *f*-MWNTs will diffuse throughout the tissue as

7 observed for other nanomaterials [31] and therefore each microglial cell will likely be exposed

8 to a limited amount of nanotubes. To ensure that microglial cells interacted with the MWNTs,

9 we favoured the CNT sedimentation by exposing cells to MWNTs in a serum free

10 environment for 2 h, following which the cell culture medium was supplemented with 12%

11 FBS. Following this single exposure to a unique dose of 10 µg/mL, we used a modified LDH

12 assay developed in our lab [32] to assess the impact of *f*-MWNTs on microglial cell viability at

13 1, 7, 14 and 28 days after the initial exposure (**Figure 2**). No effect on the viability of exposed

14 microglial cells compared to untreated cells was observed irrespective of *f*-MWNTs used or

15 time after exposure. However, a statistically significant difference was observed at day 1 for

16 ox-MWNT-NH_3^+ treated cells when compared to their respective control (untreated cells). This

17 could be ascribed to the primary nature of the cell cultures used here (more dying cells in

18 untreated cells than in ox-MWNT-NH_3^+ treated cells) [14] or to a stimulation of viability as

19 primary microglial cells preserve the ability to divide under stimulatory conditions [33]. Further

20 investigations will be needed to address this question. Overall, these results suggested that

21 microglial cells are tolerant to *f*-MWNTs exposure under the conditions used here, and that

22 this tolerance is not dependent on the type of chemical functionalisation for this

23 concentration. These results were in agreement with previous observations of a dose

24 dependent cytotoxicity appearing after 24 h above 10 µg/mL [13].

25

26 **Primary microglial cells internalised and kept nanotubes over time.** CNTs found

27 primarily free in the cytoplasm were reported to reduce proliferation and induce apoptosis in

28 BV2 cells, an immortalised model of microglial cells [18]. In order to explain the difference

29 between this study and the viability results of the present study (**Figure 2**), optical

30 microscopy was used to investigate the internalisation pattern and evolution of CNT loading

31 over time (**Figure 3a, S2 and S3**). For all three *f*-MWNTs and irrespective of the time point

32 considered, the distribution of nanotubes observed as black material in bright-field mode

33 (**Figure S2 and S3**) was characteristic, with an accumulation of materials around the nucleus

34 (perinuclear region), absence of black material in the nucleus, and no apparent accumulation

35 in the cytoplasm periphery close to the cell boundaries (**Figure S3**). No obvious difference in

36 terms of CNT loading from 1 day to 28 days was observed for all three *f*-MWNTs, suggesting

1 that exocytosis was limited. In addition, using immunocytochemistry (anti-CD68), a singular

2 pattern of CD68 immunolabelling was observed, with black materials appearing as entrapped

3 in vesicles positive for CD68 immunoreactivity (**Figure S4**). The vesicular pattern was

4 enhanced and contrasted by the black materials contained within the CD68 positive vesicles.

5 CD68 is predominantly an intracellular glycosylated transmembrane protein with minimal

6 surface expression in unactivated macrophages [34]. The perinuclear position of CNT

7 accumulation, the absence of diffuse CNT-related black signal across the cytoplasm, and the

8 vesicular pattern of CD68 immunoreactivity suggested a vesicular accumulation of *f*-MWNTs.

9   In order to confirm that the punctuated black halo around the nucleus (**Figure S5b**)

10 was indeed due to localised accumulation of carbon nanotubes, Raman spectroscopy

11 analysis was performed at a single cell level and in different places of the considered cell

12 (**Figure 3 b**). The characteristic peaks at 1360 cm^{-1} (D band), 1585 cm^{-1} (G band) and 1620

13 cm^{-1} (D' band) were used to confirm the CNT nature of the accumulation [35, 36]. Following

14 exposure to *f*-CNTs, all three microglial cell cultures exhibited the specific Raman signature

15 of MWNTs (*i.e.* D, G, D' bands) in the perinuclear region (**Figure S5b**). For each *f*-CNTs, the

16 Raman profile found in cells (**Figure 3b**) was similar to the Raman profile of the starting

17 materials used to treat the cells (**Figure S5a**), confirming the adequacy and specificity of

18 Raman fingerprints to characterise carbon nanomaterials. In addition, Raman signature of

19 MWNTs was observed at each time points tested (*i.e.* 1, 7, 14 and 28 days), confirming the

20 persisting perinuclear presence of *f*-CNTs in each case (**Figure 3b**). Taken together, these

21 results show that the type of chemical functionalisation had no influence on the

22 internalisation of *f*-MWNTs, their distribution within the cells, and their overtime retention in

23 microglial cells. However, both endocytosis and exocytosis of *f*-MWNTs in primary microglial

24 cells will need further investigations to fully describe the mechanisms and kinetic of

25 processes at stake. In particular, further studies investigating the amount of materials

26 internalised and maintained in cells over time for each *f*-MWNT considered will be important,

27 as over time degradation in microglial cells in a surface chemistry dependent manner has

28 been recently confirmed using two different methodological approaches [14, 15]. Importantly, as

29 mentioned above, the persistent retention of *f*-MWNTs over 28 days around the nucleus of

30 microglial cells had no effect on viability, which demonstrated an absence of correlation

31 between intracellular accumulation of materials and cytotoxicity under the considered

32 conditions.

33 **Uptake of *f*-MWNTs did not induce pro-inflammatory reaction in microglial cells.** Since

34 internalisation of CNTs had no effect on microglial cells viability over time, it was then

35 questioned whether the CNT uptake could induce the release of pro-inflammatory factors.

36 The Griess assay was therefore used to measure the amount of NO released by MWNT

1　exposed microglial cells at 1, 7, 14 and 28 days after the initial exposure (**Figure 4**). NO is

2　one of the main markers for microglial cell activation and pro-inflammation induction, and is

3　also a toxic agent for neurons [17, 37]. A statistically significant release of NO compared to

4　untreated cells was observed 24 h after the initial exposure to CNTs for all three *f*-MWNTs.

5　However, this positive release of pro-inflammatory markers was largely limited in comparison

6　to LPS stimulated microglial cells. At later time points, the release of NO became not

7　significant compared to untreated cells and disappeared at 28 days. These data showed that

8　*f*-MWNTs irrespective of their surface functionalisation have a limited ability to induce

9　inflammation *in vitro* under the conditions used here, and that their internalisation and

10　persistence in microglial cells over time did not lead to chronic pro-inflammatory reaction, as

11　would have been expected if microglial cells were activated and inducing an immune

12　response, as previously observed with other MWNTs [16].

13　**Uptake of *f*-MWNTs did not alter internalisation or migration abilities.** The presence of *f*-

14　MWNTs inside microglial cells for 28 days did not seem to affect their viability or to induce an

15　inflammatory reaction. The next question was then to know whether other basic physiological

16　functions characteristic of resident macrophages would stay unimpaired by *f*-MWNT

17　exposure and over-time persistence in cells.

18　　　　Firstly, the internalisation ability of CNT-laden microglial cells was tested, using 0.5

19　μm fluorescently labelled polystyrene beads. It was rationalised that if the internalisation

20　ability was maintained, the uptake of polystyrene beads for each microglial cell considered

21　would be limited only by the amount of materials (*i.e.* CNTs) already inside these MWNT-

22　preloaded cells. The internalisation of polystyrene beads inside microglia previously exposed

23　to MWNTs was assessed over 8 h and compared to naïve microglial cells (*i.e.* non-exposed

24　to MWNTs) and activated microglial cells (*i.e.* non-exposed to MWNTs but stimulated by LPS

25　(200 ng/mL)) (**Figure 5 and S6**). The internalisation assay was performed only at day 7 after

26　exposure to CNTs because it was observed that engulfment of polystyrene beads was

27　leading to acute cytotoxicity at later time points (14 and 28 days) for all cells, naïve

28　microglial cells included. This was attributed to the age of the primary cells, which have been

29　isolated from brain tissue about 1.5 months before day 14 time point. Similarly, the test was

30　not performed at day 1 after exposure to MWNTs because the cells were exposed to

31　MWNTs the day before and some free nanotubes might still be in the supernatant and would

32　be in direct competition with the polystyrene beads for internalisation. At the earliest time

33　point (1 h after the bead treatment), there was no major difference between groups, including

34　untreated cells or LPS stimulated cells (**Figure 5c and S6**). While non-statistically significant,

35　the amount of polystyrene beads (*i.e.* fluorescence) in microglial cells previously exposed to

36　oxidised MWNTs (*i.e.* both ox-MWNT and ox-MWNT-NH$_3^+$) was however lower compared to

1 untreated cells (**Figure 5c and S6)**. After 2 h, the LPS stimulation greatly enhanced the

2 polystyrene beads internalisation compared to the other groups (**Figure 5a and 5c)**. In

3 addition, the internalisation of polystyrene beads was slightly higher for microglia exposed to

4 aminated MWNTs (*i.e.* both ox-MWNT-NH_3^+ and MWNT-NH_3^+) compared to naïve microglia

5 or microglia exposed to ox-MWNT. After 8 h, there was no significant difference between the

6 various groups suggesting that all groups of cells had reached their highest loading in

7 polystyrene beads possible (**Figure 5b and 5c)**. It also suggested that despite their initial

8 CNT loading, CNT-laden microglial cells were able to internalise polystyrene beads to the

9 same extend as cells not pre-loaded with CNTs. These results showed that the

10 internalisation ability of microglial cells was not perturbed by uptake of *f*-MWNTs, irrespective

11 of the type of chemical functionalisation tested. These results also underlined the relative

12 tolerance of cells to *f*-MWNTs exposure, especially when considering non-overload non-toxic

13 doses (*i.e.* 10 µg/mL).

14   The migration ability of CNT-laden microglial cells was then tested. Following the

15 observation that unintended scratch on the plastic cell culture surface during the renewal of

16 cell culture medium was inducing migration of microglial cells toward the scratch, a specific

17 migration assay based on "scratch stimulated" migration was developed. The migration

18 assay was performed at day 7, 14 and 28 days after the initial exposure to one of the three *f*-

19 MWNTs and compared to the results with naïve microglial cells and microglial cells

20 stimulated with LPS (200 ng/mL) (**Figure 6 and S7)**. The assay was not performed on the

21 day following the exposure to CNTs as free CNTs might still be present in the supernatant

22 and perturb the assay. Unexpectedly, migration of microglial cells stimulated by LPS was

23 inhibited at all three time points tested compared to untreated cells (**Figure S7 and 6**). LPS

24 is indeed known to stimulate migration and should have acted as a positive control/stimulator

25 of migration [38]. It was previously reported that the amount of LPS used during an assay is a

26 critical parameter that can influence the motility of primary microglial cells [39]. While low (0.1

27 ng/mL) or high (100 ng/mL) concentrations were shown to have no effect on promoting

28 migration, 10 ng/mL was reported as the adjusted dose which induce higher migration

29 compared to control cells. In our case, the reduce motility of microglial cells under LPS

30 condition can possibly be explained by the deviation of normal macrophage functionalities

31 toward an activation profile dedicated to pro-inflammatory factors secretion due to overload

32 LPS dose (*i.e.* 200 ng/mL was used for both NO release and migration assay). This will

33 require further investigations to fully understand the reason of this unusual behaviour of LPS

34 stimulated microglial cells and confirming the optimal concentration of 10 ng/mL for

35 promoting migration [39].

36   As regards to *f*-MWNTs, a chemical functionalisation dependent modification of the

37 microglial cell migration ability was observed (**Figure 6**). At any time point, microglial cells

1   exposed to ox-MWNT had higher migration ability than cells exposed to aminated MWNTs

2   (*i.e.* both ox-MWNT-NH$_3^+$ and MWNT-NH$_3^+$) with MWNTs bearing both chemical functions

3   (*i.e.* ox-MWNT-NH$_3^+$) in between ox-MWNT and MWNT-NH$_3^+$. At day 7, microglial cells

4   exposed to ox-MWNT migrated to the same extend as untreated cells whereas microglial

5   cells exposed to aminated MWNTs (*i.e.* both ox-MWNT-NH$_3^+$ and MWNT-NH$_3^+$) moved less

6   than untreated cells. At day 14, surprisingly, microglial cells exposed to any type of MWNTs

7   migrated more than untreated cells. At day 28, only microglial cells exposed to oxidised

8   MWNTs (i.e. both ox-MWNT and ox-MWNT-NH$_3^+$) migrated more than untreated cells or

9   cells exposed to MWNT-NH$_3^+$, which both show similar migration ability. These results

10 showed that internalisation of *f*-MWNTs did not alter microglial cell migration ability and that

11 exposure to (and uptake of) *f*-MWNTs can actually stimulate migration ability in a chemical

12 functionalisation dependent fashion. In contrast to amination, oxidation of MWNTs seemed to

13 stimulate the migration ability. Similar enhance migration ability in comparison to untreated

14 cells has been recently observed when peritoneal macrophages were exposed to nano

15 graphene oxide flakes and to a higher extend when exposed to nano graphene oxide

16 functionalised with PEG groups [40]. In this study, enhanced cell migration was attributed to the

17 activation of the cells towards a pro-inflammatory profile upon exposure to graphene oxide

18 flakes. A correlation between enhanced cell migration and activation was not identified in the

19 present study (**Figure 4 and 6**) and would therefore require further investigations to reveal

20 the mechanism at the origin of the enhanced migration ability of cells exposed to oxidised

21 MWNTs.

22

23   In the present *in vitro* study, no activation of pro-inflammation reaction following the

24 exposure of primary microglial cells to different types of *f*-MWNTs was observed, despite the

25 over-time persistence of the nanomaterials in the cytoplasm, in vesicles (**Figure S4 and**

26 **inset of Figure S5**), and regardless of the type of surface functionalisation. These results

27 are in agreement with other *in vitro* studies performed using the BV2 microglial cell line

28 exposed to non-functionalised MWNTs, in which either cytotoxicity nor induction of

29 expression of major inflammation markers were observed despite CNT internalisation at 48 h

30 [41]. Similarly, no cytotoxicity or pro-inflammatory cytokine release or NO production were

31 observed *in vitro* in the N9 microglial cell line exposed to oxidised MWNTs despite

32 internalisation [16]. On the contrary, using similar MWNTs and similar surface functionalisation

33 (ox-MWNT-NH$_3^+$ and MWNT-NH$_3^+$), *in vivo* cortical injection of *f*-MWNTs was demonstrated

34 to induce a neuroinflammatory response that was surface chemical functionalisation

35 dependent [11]. One month after injection, the degree of oxidation of the *f*-MWNTs was

36 suggested to be a major factor driving the immune tissue response to explain the higher

1 amount of CD11b positive (microglial cell marker) and GFAP positive (astrocyte marker) cells

2 around the site of injection for animals injected with *f*-MWNTs compared to vehicle injected

3 animals.

4   In contrast to previous reports, no effects due to interaction of *f*-MWNTs with the

5 cytoskeleton were observed here. It was indeed previously speculate that if CNTs are free in

6 the cytoplasm and interacting with the cytoskeleton, eventually forming bundles with

7 microtubules and microfilaments, they could possibly rigidify cells and consequently reduce

8 both migration and phagocytosis/internalisation abilities of the cells [18]. However, both

9 internalisation and migration abilities were here found to be normal in *f*-MWNTs exposed

10 microglial cells, despite a high internalisation of materials illustrated by a black halo around

11 the nucleus region and confirmed to be made of CNTs by Raman spectroscopy. This

12 suggested that *f*-MWNTs were likely not free in the cytoplasm but in vesicular compartments,

13 which is in agreement with the microscopic results presented in **Figure 3a, S2, S3, S4 and**

14 **S5**. Secondly, this also meant that although their cytoplasm were relatively congested with

15 CNT loading, cells were still elastic enough to perform basic cytoskeleton-mediated functions

16 and especially cell migration, one of the most important cell function *in vivo* for clearance of

17 foreign materials [17, 37]. This led us to believe that *in vivo* the tested materials would probably

18 undergo brain tissue emigration through microglial cell-mediated drainage finishing in the

19 lymphatic system without harming microglial cells. However, further studies are needed to

20 address that specific hypothesis and to assess whether free *f*-MWNTs (not engulfed in any

21 brain cells) would be able to use the brain solutes elimination system (*i.e.* glymphatic

22 clearance system) [42, 43].

23   Theoretically, CNT-cytoskeleton interactions can also hamper the cytoskeleton

24 dynamics required during cell division, and therefore modify the cell cycle, which would

25 eventually lead to apoptosis. Using the dividing BV2 microglial cell model, MWNTs were

26 indeed shown to induce apoptosis at the relatively low concentration levels of 0.6 and 6

27 µg/mL (35% and 66%, respectively) [18]. Induction of apoptotic pathway was also explained by

28 cell cycle arrest due to CNT interactions with cytoskeleton molecules [18, 44]. In contrast to

29 these studies, no cell death at 10 µg/mL regardless of the time point considered was

30 observed here. Seclusion of *f*-MWNT loading in vesicular compartments over time is likely

31 the best explanation for the difference between the present results and previous reports. This

32 will require complementary investigations on the subcellular fate of *f*-MWNTs, notably to

33 confirm the nature of the vesicular compartmentalisation of the CNT content and its potential

34 dynamics (endocytosis/exocytosis) over time. Moreover, a complete dose-response

35 relationship correlated with the physicochemical features of the materials should be

36 performed in order to identify the full extent of microglial tolerance to *f*-MWNTs and its

37 limitations.

1   Degradation and clearance of cell debris and foreign materials are also a fundamental

2   role of microglial cells for maintaining brain homeostasis [17]. After stereotactic administration

3   of aminated MWNTs in the cortex of mice, resident microglial cells were reported to

4   internalise and then alter the structural integrity of the injected materials [12]. Analysis of tissue

5   sections via Raman spectroscopy and electron microscopy gave evidence of the initiation of

6   a degradative process within two days following the injection. Similarly, it was shown that

7   after 24 h, the N9 microglial cells were able to alter the graphitic structure of oxidised

8   MWNTs [16]. And finally, but more importantly using the same model as described in the

9   present study (same primary cells, same f-MWNTs, same 10 µg/mL dose), primary microglial

10   cells were showed to degrade f-MWNTs over time, irrespective of the surface

11   functionalisation of MWNTs [14, 15]. These results demonstrate that in addition to conserving

12   their internalisation and migration abilities as reported here, microglial cells had preserved

13   their degradation functions despite their CNT loading. Taken together, these results confirm

14   that microglial cells exposed to 10 µg/mL of the f-MWNTs used here are still fully functional

15   cells.

16   The agglomeration and colloidal properties of the three CNT suspensions were not

17   found to be different (**Figure S1**). Similarly, variations in the surface chemical

18   functionalisation were not found to be deterministic in the impact of the three CNTs apart

19   from the migration ability that seemed to be stimulated by the two oxidised CNTs, in an

20   oxidation degree dependent manner (ox-MWNT>> ox-MWNT-NH$_3^+$; **Figure 6**). But

21   alongside surface chemical functionalisation and agglomeration, dimensions (both length and

22   diameter) are important parameters for CNT biological impact [45-48]. In this respect, the type of

23   CNTs (multi-walled rather than single-walled or double-walled) could also be important as

24   dimensions together with agglomeration will highly differ between CNT types. Therefore, the

25   present results obtained with MWNTs are likely to be different if SWNTs would have been

26   used.

27

Conclusion

29   In summary, primary microglial cells when exposed to a low concentration of f-CNTs

30   maintained their basic resident macrophage functions (phagocytosis/internalisation,

31   migration, degradation) and did not initiate an inflammatory reaction despite a large

32   internalisation of materials in cytoplasm vesicles. Considering the key role of microglial cells

33   within the brain, the demonstration of the relative absence of bioreactivity of f-CNTs upon

34   interaction with microglial cells is an important step towards their development as

35   nanovectors for drug delivery purpose in the central nervous system.

Experimental

Materials, MWNTs and preparation of MWNT suspensions for cell exposure. Chemicals and solvents were obtained from Merck / Sigma-Aldrich (UK). Cell culture reagents (PBS, trypsin, foetal bovine serum, DMEM:F12) were purchased from Gibco (ThermoScientific, UK). Multi-walled carbon nanotubes (MWNT) were purchased from Nanostructured and Amorphous Materials Inc. (Houston, TX, USA; Lot # 1240XH, 95%). The different chemical functionalisation of the MWNTs were performed as previously reported [25, 27, 28, 32]. The amount of COOH (on both ox-MWNT and ox-MWNT-NH_3^+) after the oxidation reaction has been previously calculated using thermogravimetric analysis, corresponding to 1.7 µmol·g^{-1} [49] while the amount of amino groups measured by Kaiser's test was 170 µmol·g^{-1} for ox-MWNT-NH_3^+ and 84 µmol·g^{-1} for MWNT-NH_3^+. Preparations of f-MWNT dispersion for cell exposure were performed as previously reported [14].

Stability of f-MWNT suspension in different media assessed by UV-Vis spectrophotometry. Suspension of the three f-MWNTs originally prepared in 5% dextrose water solution (1 mg/mL) were diluted to 10 µg/mL in 5% dextrose water solution, cell culture medium (DMEM:F12) supplemented with 12% FBS or cell culture medium (DMEM:F12) without FBS. Absorbance spectra were acquired at 0 h and 24 h after preparing the different 10 µg/mL suspensions using a Cary 50 Bio UV/Vis spectrophotometer (Varian Inc., Agilent Technologies, UK). For measurement, the prepared suspensions were transferred from a microtube (0.5 mL) to a 1 mL quartz cuvette with 1 cm path length. Measurements were performed at room temperature, using a dual beam mode with baseline correction based on 5% dextrose water solution, cell culture medium with 12% FBS or cell culture medium without FBS, as blank controls to create the baseline.

Primary microglial cell cultures and exposure to functionalised CNT. The preparation of primary microglial cell cultures were performed as previously reported [14] and according to a previously described method, based on mild trypsinisation of mixed glial cell culture [50] prepared from rat embryonic stratial extracts. Microglial cell cultures were then exposed for 2 h to a non-cytotoxic 10 µg/mL CNT suspension prepared in serum free cell culture medium (DMEM:F12 medium). After 2 h incubation at 37°C without serum, the cell culture medium was completed with heat inactivated foetal bovine serum (12%). After 24 h incubation at 37°C, the supernatant containing CNTs was removed, cells were washed twice with pre-warmed PBS and then incubated with CNT free complete medium (DMEM:F12 with 12% serum) for 1, 7, 14 and 28 days (recovery periods). CNT-free complete medium was changed every 3 days.

Cell viability assess by modified LDH assay. Cell viability was assessed by a modified LDH assay as previously described [32]. The Promega Cytotox 96 © Non-radioactive cytotoxicity assay (Promega, UK) was modified to avoid interference between CNTs and LDH. DMSO 10% was used as positive control of the assay. Microglial cell cultures were generated in 24 well plates. At the desired time points (1, 7, 14 and 28 days), cells were lysed with 10 µL of lysis buffer (0.9% triton X100 in distilled water) per 100 µL serum free media and left for 45 min at 37°C. After centrifuging (13000 rpm, 5 min), 50 µL of cell lysate supernatant were mixed with 50 µL of substrate mixture in a new microtiter plate and incubated for 6 min at room temperature. LDH content was determined by reading the absorbance at 490 nm using a multiwell plate reader (Fluostar Omega, BMG Labtech Ltd.). The amount of LDH detected after cell lysis indicated the number of cells that have survived to CNT exposure. The percentage cell survival is expressed as [LDH released from tested cells - Blank (media alone) / LDH released control cells- Blank (media alone)] ×100. Each assay was performed at least 3 times, using 3 wells per conditions at each considered times.

Raman spectroscopy. A Thermo Scientific DXR Raman microscope, equipped with an Olympus microscope (100x objective lens) and a 633 nm LASER (1 mW of LASER power) was used to perform Raman spectroscopy. Collection of Raman spectra was performed as previously described [14].

14

1   **Immunocytochemistry of microglial cells.** Microglial cell cultures were prepared on poly-L-lysine
2   coated plastic tissue-culture treated dishes (35 mm diam.). At the end of exposure, cells were fixed
3   with pre-cooled methanol (-20°c) for 10 min, air-dried and then washed twice with PBS containing
4   0.1% triton (TPBS, pH 7.4) before staining. Staining with primary antibody was performed after 1 h
5   incubation (i.e. blocking) with 5% of normal goat serum in TPBS. Primary antibodies used were:
6   mouse monoclonal anti-CD11b/c (1:200)(Ox42, Abcam) or mouse monoclonal anti-CD68 (ED1,
7   Abcam, UK); both diluted in 2% BSA in TPBS and incubated for 2 h at room temperature. The
8   secondary antibody (goat anti-mouse Cy3 labelled) was used at the dilution of 1:250 in 2% BSA in
9   TPBS for 1 h at room temperature. After washing, cell preparations were mounted in appropriate
10 medium containing anti-fading agent and DAPI (Vectashield, Vector laboratories LTD).
11 Immunoreactivity was assessed on an inverted epifluorescence microscope (Carl Zeiss Axio Observer
12 A1).
13
14 **Inflammation markers (NO release) assess by Griess reagent assay.** Inflammation reaction was
15 based on the release of NO, a well-known biomarker of inflammation for microglial cells. As for the
16 cytotoxicity assay, microglial cell cultures were generated in 24 well plates. Cells were then exposed
17 to 10 μg/mL of the three different CNT suspensions or to CNT free medium. LPS (E. Coli, O26:B6, 200
18 ng/mL) was used as positive control for inflammation and was applied 24 h before performing the
19 measurement on cell supernatants. At day 1, 7, 14 and 28 after CNT exposure, the amount of nitrite
20 (stable breakdown products of NO) was measured using the Griess reagent system assay (Promega,
21 UK) following the manufacturer's instructions. In brief, 50 μl of each experimental sample was mixed
22 with 50 μl of the Sulfanilamide Solution. Following 8 min incubation, 50 μl of the NED Solution were
23 added to all wells for 8 min incubation before reading absorbance at 530 nm. The amount of nitrite
24 was determined by comparison to a nitrite standard reference curve, prepared and measured in
25 parallel to each sample measurement.
26
27 **Phagocytosis/internalisation ability assess by fluorescent polystyrene beads assay.** To assess
28 the internalisation ability of CNT-laden microglial cells, we used 0.50μm Fluoresbrite® YellowGreen
29 Microspheres (Polysiences, Inc.) and reduced the cell density of microglial cell cultures (1/2 of usual
30 cell density when preparing mixed glia cell culture). No assay was performed at day 1 after the CNT
31 exposure as some CNTs might still be present in the cell culture medium and compete with the beads
32 for internalisation, despite precautious washings. Assays were therefore performed at day 7 of the
33 recovery period. At this time point, 2 μL of the initial beads suspension was diluted in 2 mL of complete
34 cell culture medium. This bead diluted suspension was used to treat CNT-laden microglial cells
35 prepared and cultured in 35 mm cell culture dishes. The phagocytosis of the fluorescently labelled
36 beads was followed on an inverted epifluorescence microscope tuned on the FITC channel (Carl Zeiss
37 Axio Observer A1) and recorded at 1, 2 and 8 h after bead treatment. Green fluorescence present in
38 each picture was measured using ImageJ image processing and analysis software (NIH, USA).
39
40 **Migration ability assess by scratch assay.** To assess the migration ability of CNT-laden microglial
41 cells, we developed a migration assay based on the well-known wound-healing assay and using the
42 formation of scratches at the bottom of the plastic cell culture support. Using reduced cell density of
43 microglial cell cultures (1/2 of usual mixed glia cell density), we first exposed cells to 10 μg/mL of the
44 different *f*-MWNT suspension for 24 h for loading purpose. As for the internalisation assay, no
45 migration assay was performed at day 1 after CNT exposure because it was considered too soon after
46 exposure and the presence of free CNTs on the cell culture surface might bias the migration
47 assessment of CNT-laden microglial cells. On day 7, 14 and 28 of the recovery period, we generated
48 straight scratches on the plastic surface of 35 mm cell culture dishes by gently drawing straight lines
49 using a sterile plastic pipette tip. To allow a maximum number of cells to move towards the scratches,
50 migration ability was assessed 72 h after generation of the scratches. Pictures were centred on the
51 scratch and a ROI was drawn around the scratch to count the cells present in the ROI of each picture
52 (ImageJ image processing and analysis software (NIH, USA)) as illustrated in supplementary
53 information **Figure S7**.

1

2 **Statistics.** Results are expressed as mean ± SD. Statistical differences were analysed using the

3 Student's t test, and p<0.05 (*) were considered as significantly different. Each assay was performed

4 independently at least 3 times. One way ANOVA, Kruskal-Wallis test with Dunn's multiple comparison

5 test was used to analyse the differences in the viability assay p<0.05 (*) were considered as

6 significantly different.

7

8 # Acknowledgments

15

16

Figure Legends

Figure 1: Characteristics of the different types of functionalised MWNTs. (a) Chemical structures of the different chemically functionalised MWNTs; (b) Table providing the abbreviations used in the manuscript, the length and the amount of amino groups for the different MWNTs.

Figure 2: Cytotoxic effects of different MWNTs on primary microglial cell cultures evaluated by modified LDH assay. Microglial cell cultures were exposed during 24 h to a unique dose of different MWNTs (10 µg/mL). Following different period of time after the exposure, the LDH assay was performed. No significant effect was observed compared to untreated cells or positive control (DMSO 10%). One way ANOVA, Kruskal-Wallis test with Dunn's multiple comparison test was used to analyse the differences in the viability assay $p<0.05$ (*) were considered as significantly different.

Figure 3: Imaging of primary microglial cells exposed to different functionalised MWNTs via optical microscopy and confirmation of CNT via Raman spectroscopy. Primary microglial cell cultures were exposed during 24 h to a unique dose of different MWNTs (10 µg/mL) and then leaved for different period of time before imaging. (a) Live imaging (phase contrast) of primary microglial cells at day 1 to 28 for the different exposure. LPS activation (200 ng/mL) was used as a control that induced a change in cell shape (cells flattened and spreaded). No significant difference in terms of shape or number of cells was observed between the non-treated cells and the cells exposed to MWNTs at any time of recovery after the initial exposure. (b) At the end of each desired time of recovery, primary microglial cells were fixed with -20°c pre-cooled methanol and then air dried for at least one hour before further analysis. The Raman analysis of regions randomly selected within the cell boundaries was performed (as presented in **Figure S5c**). Intensities were normalised to the intensity of G band (I_G = 1). For all MWNTs and for all time points considered, the typical Raman signature of MWNTs constituted of D, G and D' bands was obtained in regions which appeared black under bright-field microscopy. No Raman signature of CNTs was detected in white regions (nucleus and cell periphery). All scale bars shown are 100 µm.

Figure 4: Inflammation reaction assessed by a measurement of NO release using the Griess reagent assay. Microglial cell cultures were exposed during 24 h to a unique dose of different MWNTs (10 µg/mL). Following different period of time after the exposure, the Griess reagent system assay was performed. No significant effect was observed compared to untreated cells or positive control (LPS 200 ng/mL). Only at day 1 after the initial CNT exposure, the NO release was higher than the untreated cells but minimal compared to the NO release induced by LPS stimulation.

Figure 5: Internalisation ability assessed by a fluorescently labelled microsphere assay. Microglial cell cultures were exposed during 24 h to a unique dose of different MWNTs (10 µg/mL). On day 7 after this initial exposure, microglial cells were treated with fluorescently labelled microspheres (0.5 µm). The internalisation of the fluorescent microspheres was recorded at 2 h (a) and 8 h (b) after the treatment. For the LPS control, untreated cells were exposed to LPS (200 ng/mL) 24 h before the microsphere treatment in order to separate LPS stimulation and microsphere exposure, as for the MWNT exposure. A quantitative measurement of the fluorescence obtained in each pictures was analysed via ImageJ and is presented in (c). For 8 h, results presented have been divided by a factor 10 for all conditions. After 1 and 8 h, no significant internalisation was observed compared to untreated or LPS stimulated cells. At 2 h following microsphere exposure, LPS stimulated cells internalised more microsphere than untreated cells. All scale bars shown are 100 µm.

Figure 6: Migration ability assessed by a scratch assay. Microglial cell cultures were exposed during 24 h to a unique dose of different MWNTs (10 µg/mL). On day 7, 14 and 28 days after this initial exposure, the plastic surface of microglial cell culture was submitted to scratches. Seventy two hours after the scratch, the amount of cells that have migrated toward the scratch was imaged and

17

1   counted using ImageJ. For the LPS control, untreated cells were exposed to LPS (200 ng/mL) 24 h
2   before the formation of scratch on the plastic surface. The migration is presented as the percentage
3   compared to untreated cells. LPS treatment was founded to inhibit the migration of microglial cells.
4   The exposure to ox-MWNTs or ox-MWNT-NH$_3^+$ were found to significantly stimulate microglial cell
5   migration at both 14 and 28 days, with ox-MWNTs having a higher stimulation than ox-MWNT-NH$_3^+$. In
6   contrast, MWNT-NH$_3^+$ showed a limited effect on the microglial cell migration ability compared to
7   untreated cells.
8
9

10 # Supplementary Figure Legends

11

12   **Figure S1: Stability of *f*-MWNT suspension in different media assessed by UV-Vis**
13   **spectrophotometry.** Stability of the three *f*-MWNTs (10 µg/mL) suspended in 5% dextrose water
14   solution (first column), in cell culture medium (DMEM:F12) supplemented with 12% FBS (second
15   column) and in cell culture medium without FBS (third column) are presented at 0 h (red spectra) and
16   24 h (blue spectra). Absorbance spectra for the suspension media are also displayed (bottom raw).
17   Each *f*-MWNT presented specific spectra in each medium. All three *f*-MWNTs showed no difference in
18   absorbance between 0 h (blue spectra) and 24 h (red spectra) when suspended in 5% dextrose or in
19   cell culture medium with 12% FBS, red spectra overlapped with blue spectra. In contrast, a clear
20   decrease in absorbance between 0 h and 24 h was observed for all three *f*-MWNTs when suspended
21   in cell culture medium without FBS. While the blue spectra were specific to each MWNT tested, a
22   similar red spectra below the blue one was observed at 24 h for all three *f*-MWNTs, suggesting
23   instability of suspensions and sedimentation of the three *f*-MWNTs when suspended in this medium.

24

25   **Figure S2: Optical microscopy of live primary microglial cells after exposure to *f*-MWNTs.**
26   Primary microglia cell cultures were imaged at 1 (a), 7 (b), 14 (c) or 28 (d) days after a 24 h treatment
27   with different *f*-MWNTs (10 µg/mL or 0 µg/mL). The same field of view is displayed after imaging under
28   either phase contrast or bright field illumination. Bright field was used to highlight black regions in cells
29   indicating the presence of carbon nanotubes. For all microglial cell cultures (exposed and non-
30   exposed), cells with either elongated, spread or round shapes were found. All scale bars shown are
31   100 µm.

32

33   **Figure S3: Optical microscopy of live primary microglia exposed to *f*-MWNTs (higher**
34   **magnification).** Primary microglia cell cultures were imaged at 1 (a), 14 (b) or 28 (c) days after a 24 h
35   treatment with different *f*-MWNTs (10 µg/mL) using a 20x objective. Higher magnification at 40x are
36   provided for MWNT-NH$_3^+$ after 7 days (d). The same field of view is displayed after imaging under
37   either phase contrast or bright field illumination. Bright field was used to highlight black regions in cells
38   indicating the presence of carbon nanotubes. All scale bars shown are 100 µm.

39

40   **Figure S4: Immunocytochemistry of *f*-MWNTs laden microglia**. Microglial cells cultures were fixed
41   with pre-cooled methanol, washed and immunostained with mouse anti-rat CD11b/c (microglial cell
42   marker) antibodies in combination with secondary anti-mouse Cy3 antibodies or with mouse anti-rat
43   CD68 (macrophage marker) antibodies in combination with secondary anti-mouse Cy3 antibodies. (a)
44   Merged images of DAPI stain with CD11b/c or CD68 immunoreactivities for the different conditions.
45   (b) Close up on *f*-MWNT laden microglial cells for the 3 different types of MWNTs tested highlighting
46   the vesicular pattern of the MWNT loading inside the cytoplasm of microglial cells. All scale bars
47   shown are 100 µm.

48

49   **Figure S5: Raman spectroscopy of starting materials before cell exposure and imaging of fixed**
50   **cells before Raman analysis**. (a) Raman spectroscopy of the three different materials used before
51   cell exposure was performed by deposing a drop of the starting 5% dextrose dispersion of MWNTs (1

1   µg MWNT/mL) on a glass slide. (b) Representative pictures of cells exposed to MWNT-NH$_3^+$ showing
2   the typical distribution of nanotubes around the nucleus and a granular accumulation pattern
3   suggesting vesicular accumulation, both in phase contrast and bright-field mode. (c) Representative
4   pictures of untreated cells or cells exposed to MWNT-NH$_3^+$ in bright-field mode at different levels of
5   magnification. Also presented is a typical map for point and shout Raman analysis.
6
7   **Figure S6: Internalisation ability assessed by a fluorescently labelled microsphere assay**.
8   Microglial cell cultures were exposed during 24 h to a unique dose of different MWNTs (10 µg/mL). On
9   day 7 after this initial exposure, microglial cells were treated with fluorescently labelled microspheres
10 (0.5 µm). The internalisation of the fluorescent microspheres was recorded at 1 h after the treatment.
11 For the LPS control, untreated cells were exposed to LPS (200 ng/mL) 24 h before the microsphere
12 treatment in order to separate LPS stimulation and microsphere exposure, as for the MWNTs
13 exposure. A quantitative measurement of the fluorescence obtained in each pictures was analysed via
14 ImageJ and is presented in Figure 3c. All scale bars shown are 100 µm.
15
16 **Figure S7: Migration ability assessed by a scratch assay**. Microglial cell cultures were exposed
17 during 24 h to a unique dose of different MWNTs (10 µg/mL). On day 7, 14 and 28 days after this
18 initial exposure, the plastic surface of cell culture was submitted to scratches (see schemes). After the
19 scratch, cells that have migrated towards the scratch was imaged (representative pictures, 72 h after
20 the scratch) and counted using ImageJ in the ROI highlighted in yellow. For the LPS control, untreated
21 cells were exposed to LPS (200 ng/mL) 24 h before the formation of scratch on the plastic surface. All
22 scale bars shown are 100 µm.

References

1. P. Blasi, S. Giovagnoli, A. Schoubben, M. Ricci and C. Rossi, *Adv Drug Deliv Rev*, 2007, **59**, 454-477.
2. T. Patel, J. Zhou, J. M. Piepmeier and W. M. Saltzman, *Adv Drug Deliv Rev*, 2012, **64**, 701-705.
3. S. B. Pehlivan, *Pharm Res*, 2013, **30**, 2499-2511.
4. J. T. Wang and K. T. Al-Jamal, *Nanomedicine (Lond)*, 2015, **10**, 2639-2642.
5. K. Kostarelos, L. Lacerda, G. Pastorin, W. Wu, S. Wieckowski, J. Luangsivilay, S. Godefroy, D. Pantarotto, J. P. Briand, S. Muller, M. Prato and A. Bianco, *Nat Nanotechnol*, 2007, **2**, 108-113.
6. Z. Yang, Y. Zhang, Y. Yang, L. Sun, D. Han, H. Li and C. Wang, *Nanomedicine-Uk*, 2010, **6**, 427-441.
7. K. T. Al-Jamal, L. Gherardini, G. Bardi, A. Nunes, C. Guo, C. Bussy, M. A. Herrero, A. Bianco, M. Prato, K. Kostarelos and T. Pizzorusso, *Proc Natl Acad Sci U S A*, 2011, **108**, 10952-10957.
8. H. J. Lee, J. Park, O. J. Yoon, H. W. Kim, D. Y. Lee, D. H. Kim, W. B. Lee, N. E. Lee, J. V. Bonventre and S. S. Kim, *Nature Nanotechnology*, 2011, **6**, 120-124.
9. M. K. Gottipati, E. Bekyarova, R. C. Haddon and V. Parpura, *Amino acids*, 2015, **47**, 1379-1388.
10. G. Tosi, A. Vilella, R. Chhabra, M. J. Schmeisser, T. M. Boeckers, B. Ruozi, M. A. Vandelli, F. Forni, M. Zoli and A. M. Grabrucker, *J Control Release*, 2014, **177**, 96-107.
11. G. Bardi, A. Nunes, L. Gherardini, K. Bates, K. T. Al-Jamal, C. Gaillard, M. Prato, A. Bianco, T. Pizzorusso and K. Kostarelos, *PLoS One*, 2013, **8**, e80964.
12. A. Nunes, C. Bussy, L. Gherardini, M. Meneghetti, M. A. Herrero, A. Bianco, M. Prato, T. Pizzorusso, K. T. Al-Jamal and K. Kostarelos, *Nanomedicine (Lond)*, 2012, **7**, 1485-1494.
13. C. Bussy, K. T. Al-Jamal, J. Boczkowski, S. Lanone, M. Prato, A. Bianco and K. Kostarelos, *ACS Nano*, 2015, **9**, 7815-7830.
14. C. Bussy, C. Hadad, M. Prato, A. Bianco and K. Kostarelos, *Nanoscale*, 2016, **8**, 590-601.
15. J. Russier, L. Oudjedi, M. Piponnier, C. Bussy, M. Prato, K. Kostarelos, B. Lounis, A. Bianco and L. Cognet, *Nanoscale*, 2017.
16. A. E. Goode, D. A. Gonzalez Carter, M. Motskin, I. S. Pienaar, S. Chen, S. Hu, P. Ruenraroengsak, M. P. Ryan, M. S. Shaffer, D. T. Dexter and A. E. Porter, *Biomaterials*, 2015, **70**, 57-70.
17. L. C. Davies, S. J. Jenkins, J. E. Allen and P. R. Taylor, *Nat Immunol*, 2013, **14**, 986-995.
18. J. C. Villegas, L. Alvarez-Montes, L. Rodriguez-Fernandez, J. Gonzalez, R. Valiente and M. L. Fanarraga, *Adv Healthc Mater*, 2014, **3**, 424-432.
19. N. V. Konduru, Y. Y. Tyurina, W. Feng, L. V. Basova, N. A. Belikova, H. Bayir, K. Clark, M. Rubin, D. Stolz, H. Vallhov, A. Scheynius, E. Witasp, B. Fadeel, P. D. Kichambare, A. Star, E. R. Kisin, A. R. Murray, A. A. Shvedova and V. E. Kagan, *Plos One*, 2009, **4**, e4398.
20. C. Bussy, M. Pinault, J. Cambedouzou, M. J. Landry, P. Jegou, M. Mayne-L'hermite, P. Launois, J. Boczkowski and S. Lanone, *Part Fibre Toxicol*, 2012, **9**, 46.
21. J. T. Wang, N. Rubio, H. Kafa, E. Venturelli, C. Fabbro, C. Menard-Moyon, T. Da Ros, J. K. Sosabowski, A. D. Lawson, M. K. Robinson, M. Prato, A. Bianco, F. Festy, J. E. Preston, K. Kostarelos and K. T. Al-Jamal, *J Control Release*, 2016, **224**, 22-32.

1   22.   H. Ali-Boucetta, K. T. Al-Jamal, D. McCarthy, M. Prato, A. Bianco and K.
2   Kostarelos, *Chem Commun (Camb)*, 2008, 459-461.
3   23.   R. Singh, D. Pantarotto, D. McCarthy, O. Chaloin, J. Hoebeke, C. D. Partidos, J. P.
4   Briand, M. Prato, A. Bianco and K. Kostarelos, *J Am Chem Soc*, 2005, **127**, 4388-
5   4396.
6   24.   A. Servant, I. Jacobs, C. Bussy, C. Fabbro, T. da Ros, E. Pach, B. Ballesteros, M.
7   Prato, K. Nicolay and K. Kostarelos, *Carbon*, 2016, **97**, 126-133.
8   25.   S. P. Li, W. Wu, S. Campidelli, V. Sarnatskaia, M. Prato, A. Tridon, A. Nikolaev, V.
9   Nikolaev, A. Bianco and E. Snezhkova, *Carbon*, 2008, **46**, 1091-1095.
10   26.   C. Gaillard, G. Cellot, S. P. Li, F. M. Toma, H. Dumortier, G. Spalluto, B. Cacciari,
11   M. Prato, L. Ballerini and A. Bianco, *Advanced Materials*, 2009, **21**, 2903-+.
12   27.   V. Georgakilas, K. Kordatos, M. Prato, D. M. Guldi, M. Holzinger and A. Hirsch,
13   *Journal of the American Chemical Society*, 2002, **124**, 760-761.
14   28.   V. Georgakilas, N. Tagmatarchis, D. Pantarotto, A. Bianco, J. P. Briand and M. Prato,
15   *Chem Commun (Camb)*, 2002, 3050-3051.
16   29.   P. Wick, P. Manser, L. K. Limbach, U. Dettlaff-Weglikowska, F. Krumeich, S. Roth,
17   W. J. Stark and A. Bruinink, *Toxicol Lett*, 2007, **168**, 121-131.
18   30.   L. Dong, C. M. Witkowski, M. M. Craig, M. M. Greenwade and K. L. Joseph,
19   *Nanoscale Res Lett*, 2009, **4**, 1517-1523.
20   31.   E. A. Salegio, H. Streeter, N. Dube, P. Hadaczek, L. Samaranch, A. P. Kells, W. San
21   Sebastian, Y. Zhai, J. Bringas, T. Xu, J. Forsayeth and K. S. Bankiewicz, *Frontiers in
22   neuroanatomy*, 2014, **8**, 9.
23   32.   H. Ali-Boucetta, K. T. Al-Jamal, K. H. Muller, S. Li, A. E. Porter, A. Eddaoudi, M.
24   Prato, A. Bianco and K. Kostarelos, *Small*, 2011, **7**, 3230-3238.
25   33.   S. Ganter, H. Northoff, D. Mannel and P. J. Gebickeharter, *J Neurosci Res*, 1992, **33**,
26   218-230.
27   34.   M. P. Ramprasad, V. Terpstra, N. Kondratenko, O. Quehenberger and D. Steinberg,
28   *Proc Natl Acad Sci U S A*, 1996, **93**, 14833-14838.
29   35.   M. S. Dresselhaus, G. Dresselhaus, R. Saito and A. Jorio, *Physics Reports*, 2005, **409**,
30   47-99.
31   36.   M. S. Dresselhaus, A. Jorio, M. Hofmann, G. Dresselhaus and R. Saito, *Nano Lett*,
32   2010, **10**, 751-758.
33   37.   K. Saijo and C. K. Glass, *Nature reviews. Immunology*, 2011, **11**, 775-787.
34   38.   T. Tajima, T. Murata, K. Aritake, Y. Urade, H. Hirai, M. Nakamura, H. Ozaki and M.
35   Hori, *J Pharmacol Exp Ther*, 2008, **326**, 493-501.
36   39.   H. Scheiblich, F. Roloff, V. Singh, M. Stangel, M. Stern and G. Bicker, *Brain Res*,
37   2014, **1564**, 9-21.
38   40.   N. Luo, J. K. Weber, S. Wang, B. Luan, H. Yue, X. Xi, J. Du, Z. Yang, W. Wei, R.
39   Zhou and G. Ma, *Nat Commun*, 2017, **8**, 14537.
40   41.   B. Kateb, M. Van Handel, L. Zhang, M. J. Bronikowski, H. Manohara and B. Badie,
41   *Neuroimage*, 2007, **37 Suppl 1**, S9-17.
42   42.   L. Xie, H. Kang, Q. Xu, M. J. Chen, Y. Liao, M. Thiyagarajan, J. O'Donnell, D. J.
43   Christensen, C. Nicholson, J. J. Iliff, T. Takano, R. Deane and M. Nedergaard,
44   *Science*, 2013, **342**, 373-377.
45   43.   J. J. Iliff, M. Wang, Y. Liao, B. A. Plogg, W. Peng, G. A. Gundersen, H. Benveniste,
46   G. E. Vates, R. Deane, S. A. Goldman, E. A. Nagelhus and M. Nedergaard, *Science
47   translational medicine*, 2012, **4**, 147ra111.
48   44.   L. Rodriguez-Fernandez, R. Valiente, J. Gonzalez, J. C. Villegas and M. L. Fanarraga,
49   *ACS Nano*, 2012, **6**, 6614-6625.

Nanoscale Horizons Accepted Manuscript

1   45.   S. Lanone, P. Andujar, A. Kermanizadeh and J. Boczkowski, *Adv Drug Deliv Rev*,
2   2013, **65**, 2063-2069.
3   46.   H. Nagai, Y. Okazaki, S. H. Chew, N. Misawa, Y. Yamashita, S. Akatsuka, T.
4   Ishihara, K. Yamashita, Y. Yoshikawa, H. Yasui, L. Jiang, H. Ohara, T. Takahashi, G.
5   Ichihara, K. Kostarelos, Y. Miyata, H. Shinohara and S. Toyokuni, *Proc Natl Acad Sci*
6   *U S A*, 2011, **108**, E1330-1338.
7   47.   C. A. Poland, R. Duffin, I. Kinloch, A. Maynard, W. A. Wallace, A. Seaton, V. Stone,
8   S. Brown, W. Macnee and K. Donaldson, *Nat Nanotechnol*, 2008, **3**, 423-428.
9   48.   C. Muhlfeld, C. A. Poland, R. Duffin, C. Brandenberger, F. A. Murphy, B. Rothen-
10   Rutishauser, P. Gehr and K. Donaldson, *Nanotoxicology*, 2012, **6**, 867-879.
11   49.   J. Russier, C. Menard-Moyon, E. Venturelli, E. Gravel, G. Marcolongo, M.
12   Meneghetti, E. Doris and A. Bianco, *Nanoscale*, 2011, **3**, 893-896.
13   50.   J. Saura, J. M. Tusell and J. Serratosa, *Glia*, 2003, **44**, 183-189.
14

ox-MWNT   ox-MWNT-NH$_3^+$ MWNT-NH$_3^+$
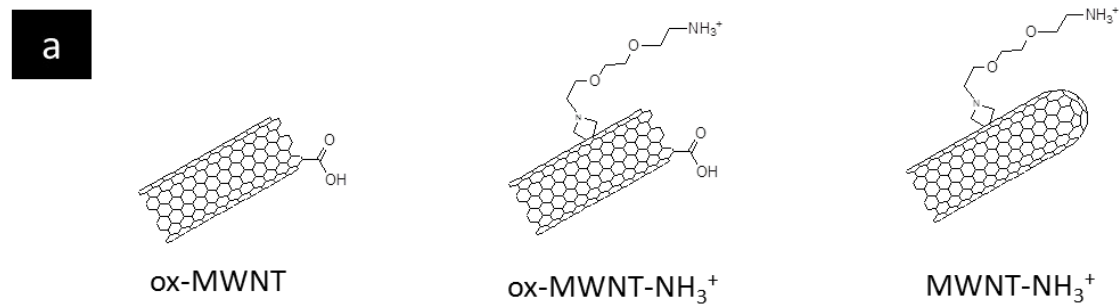
Short name	Nature of MWCNT	Amount of amino groups (Kaiser test)	Length (TEM)
ox-MWNT	carboxylated	-	200 – 300 nm
ox-MWNT-NH$_3^+$	carboxylated and aminated (cycloaddition)	170 µmol/g	200 – 300 nm
MWNT-NH$_3^+$	aminated (cycloaddition)	84 µmol/g	0.5 – 2 µm

FIGURE 1
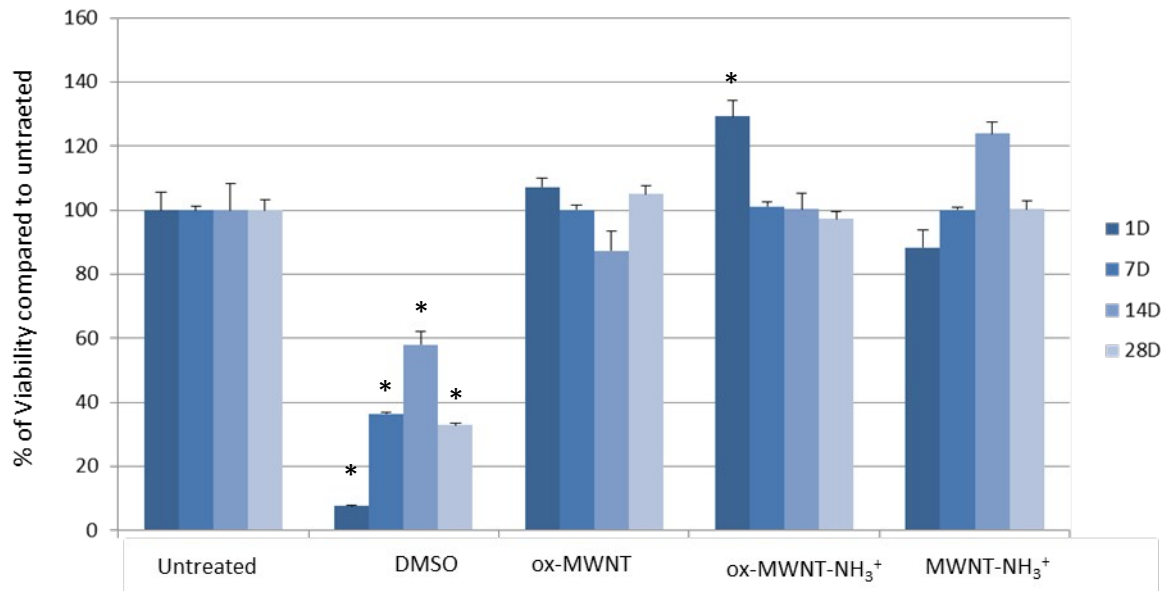
FIGURE 2

FIGURE 3

FIGURE 4

FIGURE 5

FIGURE 6